Electronic properties of electron-doped [6,6]-phenyl-C61-butyric acid methyl ester and silylmethylfullerene

Sho Furutani*, Susumu Okada**

Graduate School of Pure and Applied Sciences, University of Tsukuba, 1-1-1 Tennodai, Tsukuba, Ibaraki 305-8571, Japan

Abstract

Electronic properties of electron-doped chemically decorated C_{60} fullerenes, [6,6]-phenyl-C61-butyric acid methyl ester (PCBM) and silylmethylfullerene (SIMEF), by a planar electrode were studied using density functional theory combined with the effective screening medium method to simulate the heterointerface between the chemically decorated C_{60} and cationic counter materials. We find that the distribution of accumulated electrons and induced electric field depend on the molecular arrangement with respect to the external electric field of the electrode. We also show that the quantum capacitance of the molecule is sensitive to molecular arrangement owing to the asymmetric distribution of the accumulated electrons.

Keywords: Fullerene, PCBM, SIMEF, Electronic structure

1. Introduction

Over the past three decades, fullerenes have been keeping a premier position in nanoscale sciences and technologies, because of the diversity of their geometry and corresponding electronic properties. Fullerenes have been widely applied as starting materials for various derivatives that form constituents of devices. The structural variation of fullerene arises from

---

*TEL/FAX: +81-298535600 (ext. 8233)/+81-298535924
**TEL/FAX: +81-298535921/+81-298535924
Email addresses: sfurutani@comas.frsc.tsukuba.ac.jp (Sho Furutani), sokada@comas.frsc.tsukuba.ac.jp (Susumu Okada)

the multiple possible arrangements of twelve pentagons with various numbers of corresponding hexagons in a hollow-cage network topology [1, 2, 3]. Owing to strong correlation between the geometry of fullerenes and their electronic properties, the detailed electronic structure depends not only on fullerene cage size but also on the local atomic arrangement. For example, the electronic structures of the 24 isomers of C_{84} are completely different from each other, depending on variations in their covalent network topology, even though each isomer has the same cage size [5, 4]. It has been pointed out that the π electronic structures of fullerenes can be characterized as a spherical harmonic Y_{lm}: The electronic states associated with π electrons tend to bunch up or become degenerate with each other, reflecting their approximately spherical distribution in the fullerene cage. Thus, the π electron states are often naively regarded as an electron system confined to the spherical shell with a nanometer scale diameter [6]. In addition, fullerenes commonly possess a deep lowest unoccupied (LU) state compared with that of other carbon nanomaterials and hydrocarbon molecules, owing to the twelve pentagonal rings embedded in their cages [7]. Thus, fullerenes can act as electron acceptors for electrochemical applications.

Pristine fullerenes have a moderate chemical reactivity arising from the high curvature of the molecule and can be derivatized by covalently attaching atoms [8, 9, 10, 11] or functional groups [12, 13, 14, 15, 16, 17, 18, 19] to the cage. The spherical π electron network of fullerenes can also be modulated by chemisorption of atoms and molecules, and these derivatives are known to possess unusual electronic structures, which are completely different from those of pristine fullerenes. These materials are also of great interests as constituents for optical, optoelectronic, magnetic, and photovoltaic devices. For organic thin film photovoltaic devices, chemically decorated fullerenes act as an electron acceptor in blends with appropriate donor molecules. These devices can show large open voltages owing to the deep lowest unoccupied state of the fullerene [20, 21, 22, 23, 24, 25] and remarkable power conversion efficiency of up to 11 percent [26]. Experiments are steadily developing the structure and enhancing the performance of organic thin film photovoltaic devices based on fullerene derivatives. However, the microscopic mechanism of carrier generation and detail of the nanostructure at the heterointerfaces remain unclear. This lack of understanding motivated our study to clarify the electronic properties of electron-doped fullerene derivatives interfacing with cationic materials. Thus, in this work, we aim to clarify the electronic

2

properties of chemically decorated fullerenes at heterointerfaces with electron doping by an electrode to simulate the cationic materials, using density functional theory combined with the effective screening medium method. We considered [6,6]-phenyl-C61-butyric acid methyl ester (PCBM) and silyl-methylfullerenes (SIMEF), which are widely used as accepter molecules in organic thin film solar cells. Our calculations indicated that the distribution of accumulated electrons and the induced electric field upon electron injection are sensitive to the molecular arrangement with respect to the positively charged planar electrode, reflecting the distribution of the LU state of the PCBM and SIMEF.

2. Methods and Models

In the present work, theoretical calculations were performed using density functional theory (DFT) [27, 28] implemented in the STATE package [29]. To express the exchange correlation potential among the interacting electrons, the local density approximation was applied with the Perdew-Wang functional form fitting to the Quantum Monte Carlo results on the homogeneous electron gas [30, 31]. We used an ultrasoft pseudopotential to describe the interactions between the valence electrons and the ions generated by the Vanderbilt scheme [32]. The valence wave functions and deficit charge density were expanded by a plane-wave basis set with cutoff energies of 25 and 225 Ry, respectively. The Γ point sampling was adopted to perform the Brillouin zone integration. Structural optimization was performed until the remaining force acting on each atom was less than 5 mRy/Å. To investigate the electronic properties of an individual electron-doped molecule, each molecule was well separated from its periodic images in a cuboidal cell with lattice parameters of $a = b =$21.77 and $c =$25 Å for PCBM and $a = b =$22.03 and $c =$24 Å for SIMEF. We adopted the effective screening medium (ESM) [33] method to solve the Poisson equation including the excess electrons injected by the electrode within the framework of the DFT with the plane-wave basis set.

To simulate the PCBM and SIMEF located at the heterointerface with cationic donor molecules in an organic photovoltaic device, we considered a structural model of PCBM and SIMEF located below a planar electrode by 4.0 Å vacuum spacing simulated by an effective screening medium, which can dope electrons into PCBM and SIMEF by inducing a counter charge on the electrode surface (Fig. 1). To investigate the effect of molecular arrangement
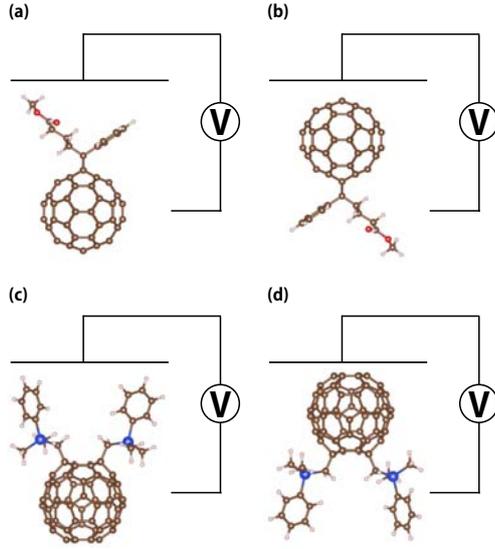
Figure 1: Schematic structures of PCBM with (a) tail-to-head and (b) head-to-tail arrangements to the electrode. Schematic structures of SIMEF with (c) tail-to-head and (d) head-to-tail arrangements to the electrode. Brown, red, blue, and white balls denote C, O, Si, and H atoms, respectively. Horizontal lines just above the fullerenes indicate the planar electrode.

on the electron accumulation, we considered two molecular orientations, the tail-to-head and head-to-tail arrangements, of PCBM and SIMEF with respect to the electrode. Under the theoretical setup, we inject up to 1 electron with a gate voltage, which corresponded approximately to 3.5 and 1.5 V for the tail-to-head and head-to-tail arrangements, respectively. During the calculations under the conditions with an excess electron, the geometries of PCBM and SIMEF were kept the same as those with zero electric field, because the forces acting on each atom were smaller than the defined criterion for the force cutoff.

3. Results and discussion

Figure 2 shows the electrostatic potential of PCBM and SIMEF without an excess electron. The electrostatic potential at the head (C_{60}) moiety is higher than that at the tail (functional groups) moiety by 0.22 and 0.23 V for PCBM and SIMEF, respectively, owing to the asymmetric shape and composition of the fullerene derivatives. This result indicates that the PCBM and
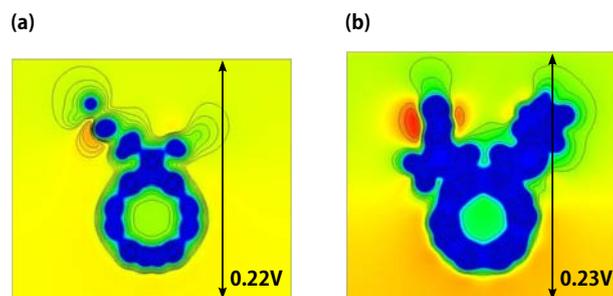
Figure 2: Contour plots of the electrostatic potential of neutral (a) PCBM and (b) SIMEF. Each contour represents higher or lower by 0.01 in the density of the adjacent contour lines.

SIMEF have an intrinsic dipole moment between the head and tail moieties, with a value of 0.60 and 0.63 D for PCBM and SIMEF, respectively. These values are smaller than those of pentamethyl C_{60} and pentaphenyl C_{60} by approximately 1.3 and 0.3 , respectively [34]. Thus, the electrostatic properties of the electron-doped molecules may be expected to be sensitive to their relative molecular arrangement with a respect to a cationic counter material, as for the case of pentaorgano C_{60} under an external electric field.
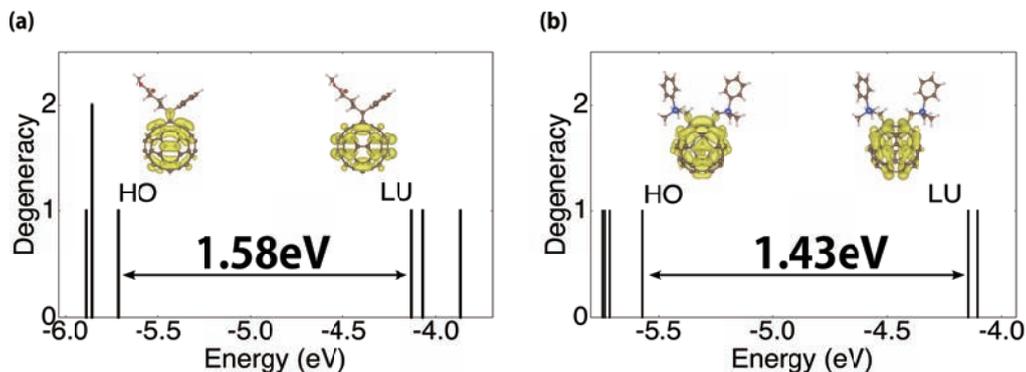

Figure 3: Electronic energy levels and isosurfaces of squared wave function of the HO and LU states of neutral (a) PCBM and (b) SIMEF. Energies are measured from that of the vacuum level.

Figure 3 shows the electronic energy levels of PCBM and SIMEF without an excess electron. The electronic structures around the Fermi level of these two molecules qualitatively exhibit the same features. The gaps between the highest occupied (HO) and LU states of the molecules were 1.58 and 1.43 eV for PCBM and SIMEF, respectively. Furthermore, the energy levels of the

5

LU state of these molecules were the same, indicating that they may give the same open voltage when used as counter donor materials in photovoltaic devices. Note that the LU state of these molecules is deeper than that of typical polycyclic hydrocarbon molecules, which are commonly used as electron donors. Thus, a sufficient charge separation may be expected to allow for the application of PCBM and SIMEF as acceptors. The similarities of the electronic structure around the HO and LU indicate that the electronic states around the gap of these molecules are associated with states distributed on the C_{60} moiety. In both molecules, the HO and LU state are distributed on the C_{60} moiety with a π electron nature, such that the injected electron is expected to be accommodated in the fullerene cage. However, these electronic states do not possess a wave function component distributed over the functional groups.
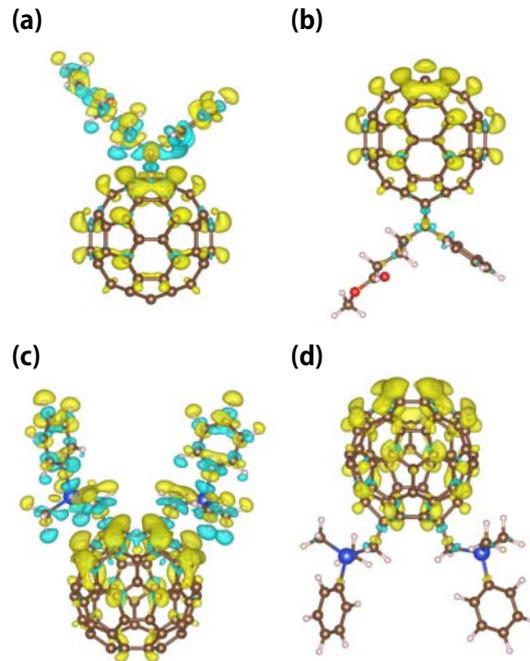

Figure 4: Isosurfaces of distribution of accumulated electrons by hole injection into the PCBM with (a) tail-to-head and (b) head-to-tail molecular arrangements, and those into SIMEF with (c) tail-to-head and (d) head-to-tail molecular arrangements, respectively. In all cases, a single electron is injected into the fullerene.

Figure 4 shows the isosurfaces of accumulated electrons in PCBM and SIMEF with two different molecular arrangements with respect to the elec-

6

trode. We find that the distribution of the accumulated electrons showed differences depending on the molecular arrangement with respect to the electrode for both fullerene molecules. However, the results did not show any dependence on the type of molecular species. The accumulated electrons localized on the C_{60} moiety of PCBM and SIMEF with a head-to-tail arrangement. In contrast, for the tail-to-head molecular arrangement, the accumulated electrons extended throughout the PCBM and SIMEF. Moreover, in this case, the accumulated carrier oscillated in the functional group owing to the charge redistribution in this region. The LU state localized C_{60} moiety can accommodate injected electrons under the head-to-tail arrangement; however, for the tail-to-head arrangement, holes in the electrode cause an electrostatic induction in the functional group moiety, which does not have wave function amplitude in low excited states, and coincidentally injects electrons into the C_{60} moiety. These findings indicate that electron injection is sensitive to the molecular arrangement with respect to the electrode. Note that the intermolecular arrangement may complicate the carrier accumulation and induced electric field, because carrier accumulation is sensitive to the molecular arrangement with respect to the electric field [35, 36].
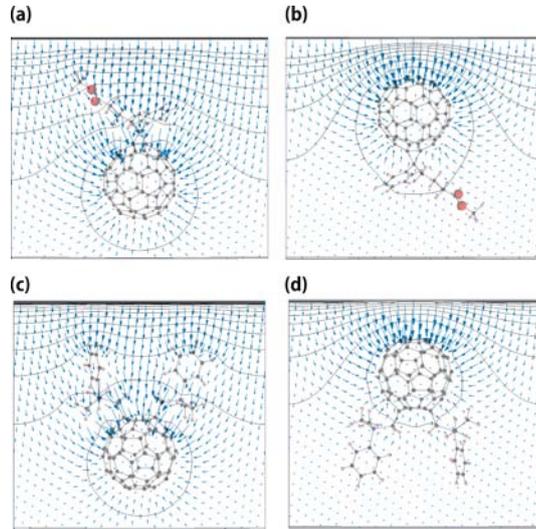

Figure 5: Contour and vector plots of electrostatic potential and electric field, respectively, of PCBM with (a) tail-to-head and (b) head-to-tail molecular arrangements, and those of SIMEF with (c) tail-to-head and (d) head-to-tail molecular arrangements, under electron doping.

7

Figure 5 shows contour plots of electrostatic potential and vector plots of the induced electric field with single electron doping. We find that the induced electric field also depends on the molecular arrangement with respect to the electrode owing to the distribution of accumulated carriers, which also depends on the molecular arrangement. For the head-to-tail arrangement with single electron doping, the electric field concentrates on the C_{60} moiety leading to a strong electric field between the molecule and the electrode for both molecules. The strong electric field is ascribed to the localized nature of accumulated electrons on the C_{60} moiety. In contrast, for the tail-to-head arrangement, the electric field is weak and extends to the C_{60} moiety, which is situated opposite to the electrode irrespective of the functional group species. Thus, the electric field between the fullerene derivatives and the donor molecules is sensitive to their relative molecular arrangement, indicating that precise control of the arrangement between the acceptor and donor molecules could further enhance charge separation at the heterointerface.
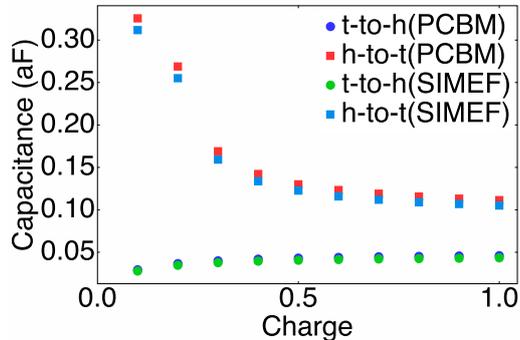

Figure 6: Quantum capacitance of PCBM and SIMEF as a function of the number of injected electrons under the tail-to-head and head-to-tail arrangements. Blue circles, red squares, green circles, and light blue squares denote the capacitances of PCBM with tail-to-head and head-to-tail, and SIMEF with tail-to-head and head-to-tail molecular arrangements, respectively.

Figure 6 shows the quantum capacitance of PCBM and SIMEF as a function of the number of electrons injected by the electrode. In both molecules the electron concentration at the C_{60} moiety caused the capacitance for the head-to-tail arrangement to be higher than that for the tail-to-head arrangement. On the other hand, the capacitance was insensitive to the functional group type, because PCBM and SIMEF both have similar electronic structures around the HO-LU gap.

8

4. Conclusions

In summary, we investigated the electronic properties of PCBM and SIMEF under an external electric field using density functional theory combined with the effective screening medium method. We find that PCBM and SIMEF have intrinsic dipole moments of 0.60 and 0.63 D, respectively, because of their asymmetric molecular shape. The LU state of the molecule is distributed on the C_{60} moiety irrespective of the functional groups attached C_{60}, so that the electronic properties are sensitive to the molecular arrangement with respect to the electrode for electron doping. The distribution of accumulated carriers and induced electric field also depend on the molecular arrangement owing to the LU state localized on the C_{60} moiety. Furthermore, the quantum capacitance of the molecule is sensitive to molecular arrangement rather than the type of molecular species. Our results give theoretical insight into the microscopic donor-acceptor interface that exists at the heterojunction of organic photovoltaic devices.

5. Acknowledgement

References

[1] M.S. Dresselhaus, G. Dresselhaus, and P.C. Eklund, Science of Fullerenes and Carbon Nanotubes, Academic Press, San Diego, CA, 1996.

[2] P.W. Fowler and D.E. Manolopoulos, An Atlas of Fullerenes, Oxford University Press, Oxford, U. K., 1995.

[3] D.E. Manolopoulos and P.W. Fowler, J. Chem. Phys. 96 (1992) 7603.

[4] B.L. Zhang, C.Z. Wang, and K.M. Ho, Chem. Phys. Lett. 193 (1992) 225.

[5] B.L. Zhang, C.Z. Wang, K.M. Ho, C.H. Xu, and C.T. Chan, J. Chem. Phys. 98 (1993) 3095.

[6] J. Sorimachi and S. Okada, Chem. Phys. Lett. 659 (2016) 1.

[7] S. Saito, S. Okada, S.-I. Sawada, and N. Hamada, Phys. Rev. Lett. 75 (1995) 685.

[8] F.N. Tebbe, R.L. Harlow, D.B. Chase, D.L. Thorn, G.C. Campbell, J.C. Calabrese, N. Herron, R.J. Young, and E. Wasserman, Science 256 (1992) 822.

[9] S.I. Troyanov, P.A. Troshin, O.V. Boltalina, and E. Kemnitz, Fullerenes Nanotubes Carbon Nanostruct. 11 (2003) 61.

[10] J.H. Holloway, E.G. Hope, R. Taylor, G.J. Langley, A.G. Avent, T.J. Dennis, J.P. Hare, H.W. Kroto, and D.R.M. Walton, J. Chem. Soc. Chem. Commun. 12 (1991) 966.

[11] R. Taylor, J.H. Holloway, E.G. Hope, A.G. Avent, G.J. Langley, T.J. Dennis, J.P. Hare, H.W. Kroto, and D.R.M. Walton, J. Chem. Soc. Chem. Commun. 9 (1992) 665.

[12] Y. Matsuo and E. Nakamura, Chem. Rev. 108 (2008) 3016.

[13] T. Akasaka, F. Wudl, and S. Nagase, Chemistry of Nanocarbons, Wiley, West Sussex, 2010.

[14] M. Sawamura, K. Kawai, Y. Matsuo, K. Kanie, T. Kato, and E. Nakamura, Nature 419 (2002) 702.

[15] Y. Matsuo, A. Muramatsu, R. Hamasaki, N. Mizushita, T. Kato, and E. Nakamura, J. Am. Chem. Soc. 126 (2004) 432.

[16] S. Okada, R. Arita, Y. Matsuo, E. Nakamura, A. Oshiyama, and H. Aoki, Chem. Phys. Lett. 399 (2004) 157.

[17] E. Nakamura, K. Tahara, Y. Matsuo, and M. Sawamura, J. Am. Chem. Soc. 125 (2003) 2834.

[18] Y. Matsuo and E. Nakamura, J. Am. Chem. Soc. 127 (2005) 8457.

[19] H. Nitta, Y. Matsuo, E. Nakamura, and S. Okada, Appl. Phys. Exp. 6 (2013) 045102.

[20] M.C. Scharber, D. Muhlbacher, M. Koppe, P. Denk, C. Waldauf, A.J. Heeger, and C.J. Brabec, Adv. Mater. 18 (2006) 789.

[21] F.B. Kooistra, J. Knol, F. Kastenberg, L.M. Popescu, W.J.H. Verhees, J.M. Kroon, and J.C. Hummelen, Org. Lett. 9 (2007) 551.

[22] Y. Matsuo, Y. Sato, T. Niinomi, I. Soga, H. Tanaka, and E. Nakamura, J. Am. Chem. Soc. 131 (2009) 44.

[23] Y. Matsuo, Chem. Lett. 41 (2012) 754.

[24] A. Sanchez-Diaz, M. Izquierdo, S. Filippone, N. Martin, and E. Palomares, Adv. Funct. Mater. 20 (2010) 2695.

[25] G. Garcia-Belmonte, P.P. Boix, J. Bisquert, M. Lenes, H.J. Bolink, A. La Rosa, S. Filippone, and N. Martin, J. Phys. Chem. Lett. 1 (2010) 2566.

[26] J. Zhao, Y. Li, G. Yang, K. Jiang, H. Lin, H. Abe, W. Ma, and H. Yan, Nature Energy 1 (2016) 15027.

[27] P. Hohenberg and W. Kohn, Phys. Rev. 136 (1964) B864.

[28] W. Kohn and L.J. Sham, Phys. Rev. 140 (1965) A1133.

[29] Y. Morikawa, K. Iwata, and K. Terakura, Appl. Surf. Sci. 169-170 (2001) 11.

[30] J.P. Perdew and Y. Wang, Phys. Rev. B 45 (1992) 13244.

[31] D.M. Ceperley and B.J. Alder, Phys. Rev. Lett. 45 (1980) 566.

[32] D. Vanderbilt, Phys. Rev. B 41 (1990) 7892.

[33] M. Otani and O. Sugino, Phys. Rev. B 73 (2006) 115407.

[34] S. Furutani and S. Okada, Appl. Phys. Exp. 9 (2016) 115103.

[35] T. Kochi and S. Okada, Appl. Phys. Exp. 9 (2016) 085103.

[36] U. Ishiyama, N.T. Coung, and S. Okada, Appl. Phys. Exp. 9 (2016) 045101.